Global Biogeochemical Implications of Mercury Discharges from Rivers and Sediment Burial

Helen M. Amos,*,[#] Daniel J. Jacob,[†,‡] David Kocman,[§] Hannah M. Horowitz,[†] Yanxu Zhang,[‡] Stephanie Dutkiewicz,[∥] Milena Horvat,[§] Elizabeth S. Corbitt,[†] David P. Krabbenhoft,[⊥] and Elsie M. Sunderland[‡,#]

[†]Department of Earth and Planetary Sciences and [‡]School of Engineering and Applied Science, Harvard University, Cambridge, Massachusetts 02138, United States

[§]Department of Environmental Sciences, Jožef Stefan Institute, 1000 Ljubljana, Slovenia

[∥]Center for Global Change Science, Massachusetts Institute of Technology, Cambridge, Massachusetts 02139, United States

[⊥]U.S. Geological Survey, Middleton, Wisconsin 53562, United States

[#]Department of Environmental Health, Harvard School of Public Health, Boston, Massachusetts 02115, United States

Ⓢ Supporting Information

ABSTRACT: Rivers are an important source of mercury (Hg) to marine ecosystems. Based on an analysis of compiled observations, we estimate global present-day Hg discharges from rivers to ocean margins are 27 ± 13 Mmol a^{-1} (5500 ± 2700 Mg a^{-1}), of which 28% reaches the open ocean and the rest is deposited to ocean margin sediments. Globally, the source of Hg to the open ocean from rivers amounts to 30% of atmospheric inputs. This is larger than previously estimated due to accounting for elevated concentrations in Asian rivers and variability in offshore transport across different types of estuaries. Riverine inputs of Hg to the North Atlantic have

Regional changes in riverine discharges of mercury since the 1970s

decreased several-fold since the 1970s while inputs to the North Pacific have increased. These trends have large effects on Hg concentrations at ocean margins but are too small in the open ocean to explain observed declines of seawater concentrations in the North Atlantic or increases in the North Pacific. Burial of Hg in ocean margin sediments represents a major sink in the global Hg biogeochemical cycle that has not been previously considered. We find that including this sink in a fully coupled global biogeochemical box model helps to balance the large anthropogenic release of Hg from commercial products recently added to global inventories. It also implies that legacy anthropogenic Hg can be removed from active environmental cycling on a faster time scale (centuries instead of millennia). Natural environmental Hg levels are lower than previously estimated, implying a relatively larger impact from human activity.
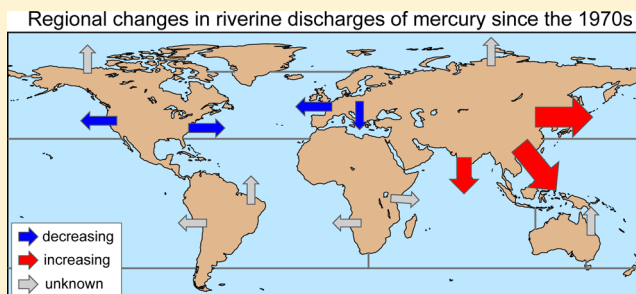
■ INTRODUCTION

Human exposure to methylmercury (MeHg), a potent neurotoxin, is primarily through consumption of marine fish.[1] Anthropogenic mercury (Hg) is transported globally by the atmosphere[2−4] and the oceans,[5] resulting in worldwide contamination. Most regulatory assessments for Hg have focused on atmospheric emissions and their subsequent fate in the global environment through deposition.[6,7] On a global scale, anthropogenic Hg releases to aquatic systems and the impact of rivers as a source to the marine environment have been understudied. Previous studies suggested that 5−15 Mmol a^{-1} of Hg is presently discharged from rivers to ocean margins,[8,9] compared to 26 Mmol a^{-1} to oceans from atmospheric deposition.[10] An estimated 90% of this Hg is buried in sediments at ocean margins (estuaries and the continental shelf).[11,12] Rivers have recently been hypothesized to be important contributors to the Hg budgets of the North Atlantic[13] and Arctic Oceans.[14−16] Here we construct a global,

spatially resolved inventory of Hg discharges from major rivers for present day, including updated information on the fraction reaching the open ocean, and estimate trends between the 1970s and present. We use global Hg models to examine the impacts of rivers on the marine environment and biogeochemical cycling.

Prior estimates of global discharges of Hg to oceans from rivers have ranged between 5 and 15 Mmol a^{-1}.[1,8,9] AMAP/UNEP[6] produced a gridded version of the inventory developed by Sunderland and Mason[8] for discharges to major ocean basins. Benthic sediments at ocean margins serve as a sink for most of this river-derived Hg[17,18] because more than 80% of Hg in rivers is bound to particles (e.g., see ref 19) and is buried in

Table 1. Mean Present-Day Riverine Hg Concentrations[a]

	mean ± SE (range)		
ocean basin[b]	[Hg(D)] (pM)	[Hg(P)] (nmol g^{-1})[c]	n[d]
Arctic			
Canada and USA	6.8 ± 1.7 (2.5−17)	0.37 ± 0.32 (0.01−0.63)	7
Russia	8.5 ± 0.9 (1.5−5.0)	0.46 ± 0.38 (0.03−0.30)	4
North Atlantic			
Europe	9.1 ± 2.1 (0.10−390)	0.49 ± 0.42 (0.40−35)	3
Canada and USA	8.7 ± 5.7 (1.8−17)	0.47 ± 0.32 (0.40−8.9)	4
South Atlantic			
South America[e]	28 ± 18 (0.50−330)	1.5 ± 1.2 (0.20−2.5)	2
Africa[f]	2.0 ± 1.3 (n/r)	0.11 ± 0.10 (n/r)	1
North Pacific			
Canada and USA	6.4 ± 3.2 (2.6−10)	0.34 ± 0.33 (0.55−7.7)	3
China	110 ± 55 (5−3000)	5.9 ± 5.8 (1.8−25)	3
South Pacific			
Southeast Asia[g]	3.6 ± 2.3 (3.2−55)	0.19 ± 0.19 (0.3−0.5)	1
South America[h]	28 ± 18 (0.50−330)	1.5 ± 1.2 (0.60−2.5)	−
China[i]	110 ± 55 (5−3000)	5.9 ± 5.8 (1.8−25)	−
Indian			
India[j]	50 ± 33 (56−370)	2.7 ± 2.9 (15−17)	1
Southeast Asia[k]	3.6 ± 2.3 (3.2−55)	0.19 ± 0.19 (0.3−0.5)	−
Africa[f]	2.0 ± 1.3 (n/r)	0.11 ± 0.10 (n/r)	1
Mediterranean[l]	1.8 ± 0.8 (1.8−120)	0.10 ± 0.09 (0.30−25)	4

[a]Flow-weighted mean dissolved concentrations [Hg(D)] are based on a survey of published measurements collected in rivers flowing into estuaries. The complete compilation of observations is in Table S1 (Supporting Information). The standard error on the weighted mean (SE)[79] is calculated when $n \geq 3$ and ranges from 30% to 65%. When $n < 3$, we assume SE = 65%. See text for estimation of [Hg(P)]. The SE of [Hg(P)] is calculated by propagating the relative SE values of [Hg(D)] and of the partition coefficient K_D in quadrature. The ranges for both [Hg(D)] and [Hg(P)] are based on reported observations (Table S1, Supporting Information). [b]Observations are aggregated by continental regions flowing into each ocean basin (indented). Ocean basin boundaries are given in Figure S1 (Supporting Information). [c]Per gram dry weight suspended sediment. [d]Number (n) of estuarine regions used to calculate the flow-weighted mean. [e]South American mean Hg concentrations are also applied to Central America. [f]Based on data for the Nile River.[34] [g]The original publication[80] only provides a range. We use the midrange value as estimate of the mean. [h]Based on observations for South American rivers entering the South Atlantic. [i]Based on observations for Chinese rivers entering the North Pacific. [j]Limited observations available suggest that rivers are highly contaminated ([Hg(D)] = 50−400 pM (Ram et al.[32]) and [THg] = [Hg(D)] + [Hg(P)] > 6000 pM[58]). We use [Hg(D)] = 50 pM as a conservative estimate. [k]Based on observations for Southeast Asian rivers entering the South Pacific. [l]Based on rivers draining from the European continent and the Nile River (Table S1, Supporting Information). Ranges not reported ("n/r").

deltas, estuaries, and on the continental shelf before reaching the open ocean.[11] However, the fraction of the suspended particle load in rivers that is buried is highly variable depending on freshwater discharge rates and the physical characteristics of different estuaries.[20] Here we use a classification scheme for export of particles from major estuarine types[21] to better estimate the fraction of particle-bound Hg reaching the open ocean and the global biogeochemical implications of Hg sequestration in ocean margin sediments.

Vertical seawater profiles from the upper ocean (1000 m) near Bermuda indicate a large (>5 pM) decrease in Hg concentrations between 1983 and 2008,[22−24] which Soerensen et al.[13] postulated could be explained by a declining source of Hg from rivers. Sediment core data from estuarine river mouths in Europe and North America support a decline in Hg discharges from many rivers since the 1970s due to decreases in commercial Hg use, environmental regulations, and wastewater treatment.[25−30] Conversely, sediment cores and inventories in China and India suggest that Hg discharges from rivers are increasing.[31−33] Seawater Hg concentrations in the North Pacific Ocean may also have increased between the late 1980s and 2006.[5] Here we combine improved estimates of Hg discharges from rivers and their temporal trends with an ocean general circulation model to estimate the plausible role of rivers in driving Hg concentrations in different ocean basins between the 1970s and present.

METHODS

Riverine Discharge of Hg to the Oceans. We construct a global, spatially distributed estimate of present-day riverine inputs to coastal margins using published measurements collected at or near river mouths (Table S1, Supporting Information). We restrict observations to the year 2000 and later, with the exception of Po, Rhone, and Nile rivers in the Mediterranean[34] where data are only available from the early 1990s. Since measurements of Hg in rivers are limited, we aggregate data by continent and ocean basin to calculate flow-weighted mean dissolved concentrations [Hg(D)] for rivers draining into each ocean basin (Table 1). Fewer measurements of suspended particle Hg concentrations are available, so mean concentrations [Hg(P)] are estimated from a partition coefficient $K_D = [Hg(P)]/[Hg(D)]$, where [Hg(P)] is in units of picomoles per kilogram of suspended particulate matter and [Hg(D)] is in units of picomoles per liter of river water. From the compilation of data in Table S1 (Supporting Information), we calculate $\log_{10} K_D = 4.7 \pm 0.3$. [Hg(P)] values estimated using this K_D fall within observed ranges (Table 1).

We multiply the resulting mean riverine Hg(D) and Hg(P) concentrations by gridded freshwater discharge and suspended sediment data to estimate annual Hg loads entering coastal marine systems (Table 2). Data on total suspended solids

Table 2. Present-Day Discharges to Ocean Margins

ocean[a]	freshwater discharge, Q[b] (km^3 a^{-1})	total suspended sediment flux, TSS[c] (Tg a^{-1})	riverine Hg(D) input[d] ($Mmol$ a^{-1})	riverine Hg(P) input[e] ($Mmol$ a^{-1})	fraction of Hg(P) reaching open ocean[f]
Arctic	3500	260	$2.9 \times 10^{-2} \pm 4.0 \times 10^{-3}$	$7.5 \times 10^{-2} \pm 6.0 \times 10^{-2}$	0.17
North Atlantic	4600	330	$3.2 \times 10^{-2} \pm 1.6 \times 10^{-2}$	0.16 ± 0.13	0.11
South Atlantic	15 000	4000	0.33 ± 0.21	5.0 ± 4.0	0.31
North Pacific	4600	2400	0.33 ± 0.16	10 ± 9.5	0.28
South Pacific	4700	4700	0.10 ± 0.06	8.5 ± 8.0	0.19
Indian	3600	3500	0.04 ± 0.02	2.5 ± 2.5	0.29
Mediterranean[g]	800	680	$1.4 \times 10^{-3} \pm 5.0 \times 10^{-4}$	0.07 ± 0.05	0.16
Southern Ocean[h]	230	180	$6.4 \times 10^{-3} \pm 4.2 \times 10^{-3}$	0.26 ± 0.20	0.48
global	37 000	16 000	0.87 ± 0.29[i]	27 ± 13[i]	0.28[j]

[a]Geographical boundaries from Figure S1 (Supporting Information). [b]Dai et al.[38] [c]ISSLCP II (http://daac.ornl.gov/ISLSCP_II/islscpii.shtml).[35] [d]Product of [Hg(D)] and Q, where [Hg(D)] is from Table 1 and has units of pM. The error on individual basins reflects ±1 standard error (SE) on [Hg(D)]. Errors for individual ocean basins are added in quadrature to estimate the error on global total Hg(D) inputs. [e]Product of [Hg(P)] and TSS, where [Hg(P)] is from Table 1 and has units of nmol g^{-1}. [f]Based on the Walsh and Nittrouer[21] classification scheme for dispersal of suspended sediment and observations from rivers belonging to each major class (see the Methods section). [g]Includes the Black Sea, assuming the same Hg(D) and Hg(P) concentrations as for the Mediterranean (Table 1). [h]Hg inputs based on riverine concentrations in South America, which contribute most of total Q and TSS inputs. [i]Errors for individual ocean basins are added in quadrature to estimate the error on global total Hg inputs. [j]Global total is weighted by Hg(P) inputs and associated export fraction in each basin.

Table 3. Enrichment Factors Relative to 2008 for Riverine Hg Inputs to Oceans[a]

ocean	1970	1980	1990	2000	2008
North Atlantic					
Europe	10 (5–14)	5 (2–7)	2 (2–3)	1 (1–2)	1
North America	8 (4–30)	3 (1–4)	2 (1–3)	1 (1–2)	1
North Pacific					
North America	4 (2–6)	2 (1–3)	1 (1–2)	1 (1–2)	1
China	0.7 (0.3–1)	0.6 (0.3–0.9)	0.8 (0.4–1)	0.9 (0.5–1)	1
Indian Ocean					
India	0.2 (0–0.6)	0.3 (0.1–1)	0.4 (0.1–2)	0.7 (0.2–3)	1
Mediterranean	5 (2–7)	2 (2–3)	1 (1–2)	1 (1–2)	1

[a]Best estimates and observational ranges from estuarine sediment cores collected at the mouths of major freshwater tributaries and riverine Hg concentration time series. See the Supporting Information for details.

(TSS) loads have a 2° × 2.5° horizontal resolution,[35−37] and freshwater discharge data (Q) have a 1° × 1° horizontal resolution.[38] Dissolved organic carbon (DOC) and particulate organic carbon (POC) were not suitable as alternate proxies for Hg(D) and Hg(P) in industrialized or contaminated systems where there are large anthropogenic inputs of Hg independent of DOC.

The fraction of Hg(P) transported beyond the continental shelf to open marine waters varies among ocean basins and is estimated from a classification system for sediment dispersal developed by Walsh and Nittrouer[21] and adapted by Zhang et al.[39] Walsh and Nittrouer[21] categorized estuaries into five types of dispersal systems based on river, wave, tide, and margin characteristics. Zhang et al.[39] used data on suspended sediment export for representative rivers in each estuary type to estimate the fraction of particle-bound Hg that reaches the open ocean.

We also considered point sources located on coastlines and discharging Hg directly to coastal waters by isolating coastal grid cells in the AMAP/UNEP[6] global 2010 inventory of anthropogenic releases to water (0.5° × 0.5° horizontal resolution). We discarded any cells overlapping with river mouths to avoid double counting. Although coastal point source discharges can be important locally (e.g., Minamata Bay[40]), we find that they are negligible globally (<0.01 Mmol a^{-1}) and do not discuss them further.

Temporal changes in Hg inputs from rivers to estuaries between the 1970s and present are estimated using dated sediment core data from estuarine river mouths. Time series of Hg concentrations in estuarine river mouths are used as available. No reliable environmental measurements with temporal information are available for India, so we estimate the change in recent decades based on a country-specific inventory for Hg.[33] All available observations and associated temporal patterns are provided in the Supporting Information. Table 3 summarizes regional Hg enrichment factors (EFs) and their upper and lower bounds used to scale present-day discharges. We assume Hg discharges have been constant at present-day levels since the 1970s in regions with no temporal information.

Three-Dimensional Ocean Model. We use the MIT global three-dimensional ocean general circulation model (MITgcm)[41] to examine the spatially variable impact of 1970s to present changes in riverine discharges on seawater Hg concentrations. The Hg simulation in the MITGCM was developed by Zhang et al.[39] It includes air−sea exchange, redox reactions, and sorption to particles following Soerensen et al.[42] in the surface mixed layer and Zhang et al.[43] in subsurface and deep waters. Particle dynamics driving settling of organic carbon (and Hg) are from the biogeochemical/ecosystem model embedded within the MITgcm.[44] The model horizontal resolution is 1° × 1° with 23 vertical levels between the ocean surface and the seafloor. The physical circulation model is constrained to be consistent with altimetric and hydrographic observations (the Estimating Circulation and Climate of the
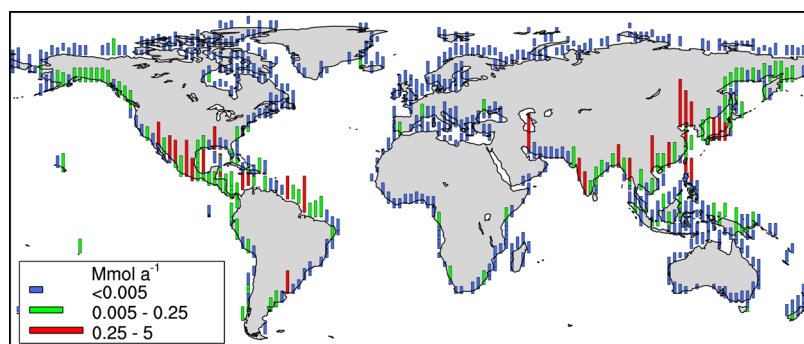
Figure 1. Present-day annual discharges of total (dissolved + particulate) mercury to ocean margins from rivers.

Ocean (ECCO) state estimates[45]). To isolate the impact of rivers, we initialize seawater Hg concentrations at zero and shut off atmospheric deposition. We then perform two separate 10 year simulations, one forced by present-day Hg discharges from rivers and the other by 1970s inputs. Ten years is selected because our estimated river Hg discharges to the North Atlantic and North Pacific vary decadally and this is also sufficient time for ocean margin sources to be transported to the open ocean. Conclusions drawn from the MITgcm remain the same with 20 year simulations.

Global Biogeochemical Box Model. We examine the longer-term impact of rivers on the full global biogeochemical cycle of Hg using an updated version of the 7-box model developed by Amos et al.,[46] which interactively couples the ocean, atmosphere, and terrestrial ecosystems. Mercury is cycled between reservoirs representing the ocean (surface, subsurface, deep), atmosphere, and terrestrial environment (fast, slow, armored pools) and is ultimately removed by burial of marine sediments. Sediments are compacted and subducted to the lithosphere, eventually returning Hg to surface reservoirs by erosion and volcanism on geologic time scales. Exchange of mass between reservoirs is described by first-order rate coefficients. The model is initialized from a natural steady-state simulation without anthropogenic Hg releases and then forced with all-time (2000 BC to 2008 AD) anthropogenic atmospheric emissions from Streets et al.[47] and additional 1850−2008 atmospheric emissions from commercial Hg use.[48] We decrease the terrestrial rate coefficients for loss to the atmosphere via photoreduction and microbial respiration of organic matter by a factor of 10, based on recent field data indicating greater Hg retention by soils.[49−51]

Amos et al.[46] treated riverine discharges as a first-order process transferring Hg from the terrestrial reservoirs to the surface ocean. The rate coefficient was based on the estimated mass of Hg from rivers that reaches the open ocean (1.9 Mmol a^{-1}) from Sunderland and Mason.[8] A term representing sequestration in ocean margin sediments was not included. We account for burial in ocean margin sediments here, which represents an important sink for anthropogenic Hg. Of the total Hg discharged at river mouths, 28% is transferred to the surface ocean, and 72% is removed to ocean margin sediments (Table 2). We view this removal to ocean margin sediments as a permanent Hg sink in the natural biogeochemical cycle in the same way as deep ocean sediments.

We further differentiate between (1) primary anthropogenic Hg directly released to a river or its watershed by human activity versus (2) erosion and terrestrial runoff of atmospherically deposited. The latter is estimated based on Hg

concentrations measured in Arctic rivers (Table S1, Supporting Information;[19,52,53]), assumed to be unimpacted by direct anthropogenic Hg releases. Extrapolated globally this amounts to 3.7 Mmol a^{-1}, which is comparable to AMAP/UNEP[6] (range 0.85−3.0 Mmol a^{-1}). From this we infer a first-order rate coefficient for loss of Hg from terrestrial ecosystems to ocean margins by rivers. Additional measurements in pristine regions (including midlatitude and tropical rivers) would help to refine these estimates/rate coefficients. Between the 1970s and present, total Hg discharges to ocean margins from rivers are constrained by observations (Tables 2 and 3). Between 1850 and 1970, we scale total Hg discharges from rivers using the historical inventory of global releases to water from commercial Hg use.[48] The primary anthropogenic contribution is calculated by difference between total discharges and erosion/terrestrial runoff and treated as an external forcing. All rate coefficients for the updated box model are provided in Table S2 (Supporting Information).

■ RESULTS AND DISCUSSION

Global Riverine Inputs and Trends. We estimate a global present-day Hg input of 27 ± 13 Mmol a^{-1} from rivers to coastal margins (Table 2). This is larger than the previous estimates of 5−15 Mmol a^{-1} and is driven by recently published data suggesting greater contamination in Asian rivers.[31,32,54−58] The uncertainty in our final estimate, expressed as a standard error on the mean, is driven by the sparsity and large variability in measured Hg concentrations in rivers (e.g., see ref 59). Riverine Hg inputs to the margins of the Pacific and Indian Oceans account for 80% of our global total (Table 2). Our estimates of discharges to ocean margins of the Atlantic, Arctic, and Mediterranean are within the ranges of previously published values.[8,14,16,34,60,61]

Figure 1 illustrates the spatial distribution of our present-day riverine inputs of total Hg to ocean margins, which is driven by both variability in Hg(P) concentrations (Table 1) and suspended sediment discharges.[35] Major rivers and highly contaminated systems are prominent (e.g., Yangtze, Amazon, Ganges). Large Hg discharges from Mexican rivers to the Pacific Ocean reflect high TSS values. Discharges from remote Asian rivers draining to the North Pacific Ocean in Figure 1 are based on observations from major Chinese rivers and may be overestimated. Discharges from African rivers are based solely on the Nile due to the absence of other Hg data. Measurements from the Congo River, due to its size and known contamination from unregulated discharges from chemical industries, leaching from solid waste dumps, and artisanal gold mining,[6,62] would be helpful for refining estimates in this region of the world.

-0.5 -0.25 -0.1 -0.05 -0.01 0 0.01 0.05 0.1 0.25 0.5 [pM]
1970-present difference in total dissolved Hg
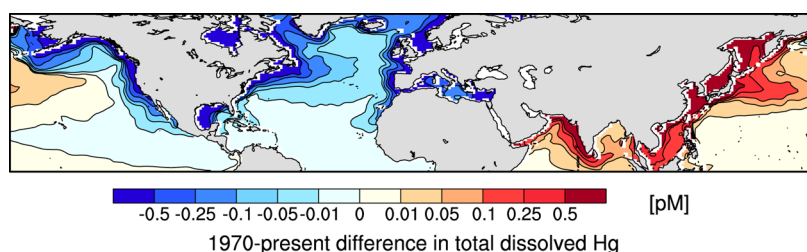
Figure 2. Simulated change in the riverine contribution to annual mean dissolved Hg concentrations in the surface ocean (0−55 m). Results are from decadal simulations with the MITgcm ocean general circulation model for the 1970s and present day. Red indicates an increase in oceanic Hg from the 1970s to present, and blue indicates a decrease.
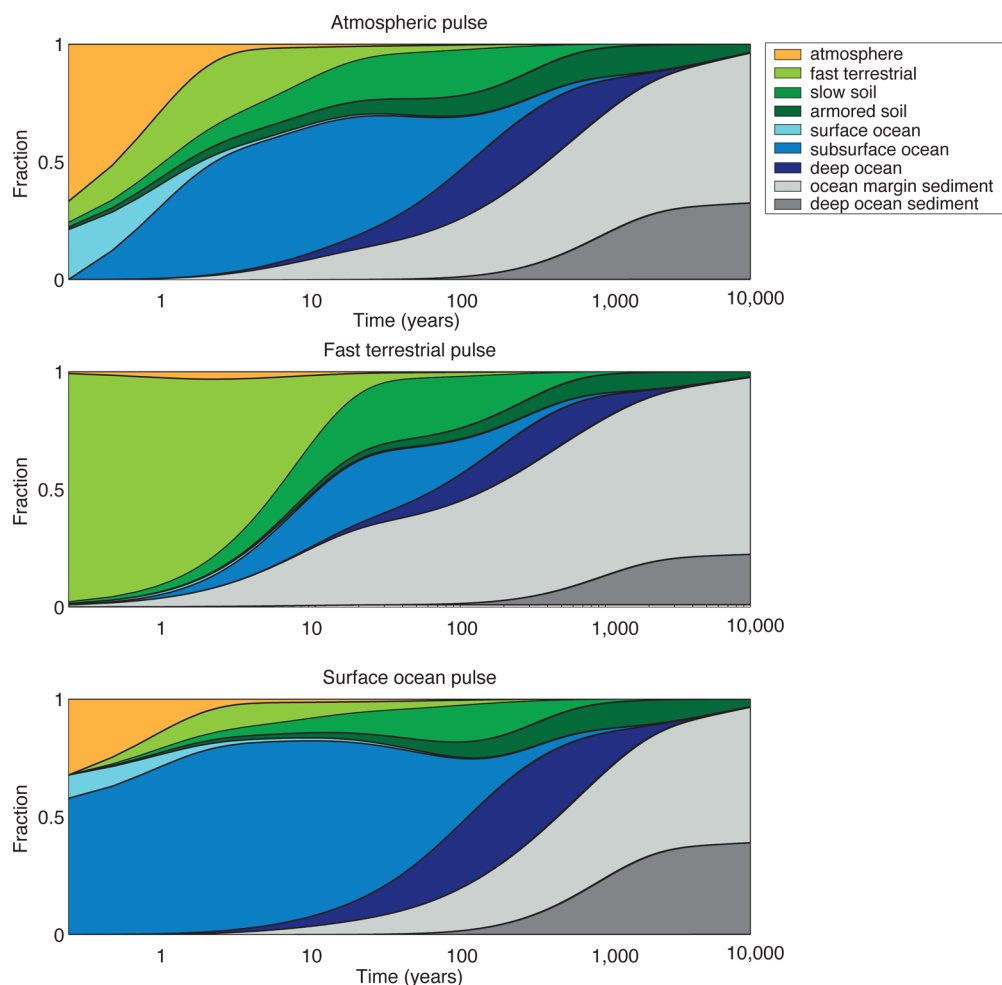
Figure 3. Time-dependent fate of a unit pulse of Hg emitted to the atmosphere at time $t = 0$ and then tracked by our global biogeochemical box model as it cycles between the ocean, atmosphere, and terrestrial reservoirs before eventually being removed to ocean margin and deep sea sediments. This figure updates the top panel of Figure 6 of Amos et al.[46]

We estimate that 28% of particle-bound Hg in rivers is exported to the open ocean globally (Table 2), a substantial increase from the 10% suggested in Sunderland and Mason[8] The export fraction is higher for the North Pacific (29%) than for the North Atlantic (11%) due to a greater prevalence of large rivers that efficiently transport suspended particles offshore.[63,64] We estimate 7.7 ± 3.8 Mmol a^{-1} of Hg discharged by rivers is delivered to the open ocean. The uncertainty is estimated by adding the errors in discharge at coastal margins for individual ocean basins in quadrature, scaled by the corresponding export fractions (Table 2). Our best estimate

(7.7 Mmol a^{-1}) amounts to ∼30% of present-day atmospheric Hg(0) and Hg(II) deposition to the oceans (26 Mmol a^{-1}).[10]

Fisher et al.[14] suggested that the summer peak in Arctic atmospheric Hg could be explained by evasion from the Arctic Ocean, which in turn might be explained by seasonal discharges of Hg from rivers. Their estimate for river discharges to the open Arctic Ocean (0.4 Mmol a^{-1}) exceeds the estimate presented here (0.04 Mmol a^{-1}). Fisher et al.[14] found that their estimate was strongly dependent on the assumed rate of Hg removal from the ocean mixed layer via particle sinking. Future efforts to refine the Hg budget for the Arctic need to resolve the coupled role of carbon and Hg cycling in the upper ocean.

Mason et al.[23] assumes 5−10% of the riverine total Hg discharged to the open ocean is present as MeHg. Subsurface water column production of MeHg is much greater than riverine inputs;[5,65−67] thus, changes in the global MeHg budget are not likely to be substantially affected by our updated estimates of total Hg discharges.

Discharges of Hg are decreasing in North American and European rivers but increasing in India and China. Mercury discharges from rivers to the margins of the North Atlantic Ocean peaked around the 1970s, likely due to the large quantities of Hg used and released from commercial products and industrial manufacturing at that time.[48,68−70] Sediment core data suggest that Hg discharges from rivers bordering the North Atlantic in the 1970s were a factor of 9 (range 4−20) larger than at present (Table 3). In India and China, riverine Hg discharges to the marine environment have increased by 40−400% since the 1970s based on sediment core data and country-level inventories of Hg releases to water.[31,33,71] The increase is likely driven by dense development and urbanization along major rivers,[31,72,73] greater use of Hg in industrial processes (e.g., in vinyl chloride monomer production),[74,75] and increasing agricultural application of Hg-containing phosphate fertilizers.[76]

Figure 2 shows the changes in riverine contributions to total dissolved Hg in the surface ocean (0−55 m) as simulated by the MITgcm given 1970s and present discharges. Results for subsurface waters (100−500 m) are shown in Figure S2, Supporting Information. Concentrations of Hg in seawater have decreased throughout the North Atlantic but increased over much of the North Pacific. The trends driven by rivers are large in coastal areas (>1 pM) but fall to less than 0.1 pM in the open oceans. Soerensen et al.[13] suggested that decreasing inputs of Hg to the North Atlantic from rivers might explain the observed 5 pM decline in seawater Hg concentrations over a 1000 m vertical profile near Bermuda between 1979 and 2008.[23] In the North Pacific, Sunderland et al.[5] reported an increase in Hg concentrations in vertical profiles measured between 1987 and 2006. The increase in North Pacific seawater is likely attributable to atmospheric deposition.[5] By contrast, Soerensen et al.[13] showed atmospheric deposition cannot explain the 5 pM decline reported near Bermuda, and our results show rivers also do not contribute substantially to these changes.

Broader Biogeochemical Implications. We use our global biogeochemical box model to examine the impacts of river discharges over longer time scales and across all geochemical reservoirs. Cumulative anthropogenic Hg forcings since 1850 include 1600 Mmol emitted to the atmosphere (1100 Mmol from ref 47, and an additional 550 Mmol from ref 48) plus 1900 Mmol of primary anthropogenic Hg discharged into rivers that flow into the ocean. Sequestration of Hg in ocean margin sediments in the model provides a sink of 1300 Mmol for anthropogenic Hg since 1850. Assuming permanent burial, we estimate that ocean margin sediments have sequestered one-third of post-1850 anthropogenic Hg releases. Removal of Hg to ocean margin sediments and decreased soil re-emissions helps balance the increase in anthropogenic sources from Horowitz et al.[48] Our simulated present-day atmosphere is 27 Mmol compared to 23−28 Mmol supported by observations;[46] the upper ocean (0−1500 m) Hg concentration is 1.7 pM compared to the range in mean total Hg across ocean basins 0.6−2.9 pM,[23] and storage in organic soils is 1200 Mmol compared to >1500 Mmol from Hararuk et

al.[49] Further increasing modeled Hg retention in terrestrial reservoirs requires a revision of the rates of Hg exchange between soil pools.

Figure 3 shows the time-dependent fate of a pulse of Hg emitted to the atmosphere in our updated model and then cycled through the different model reservoirs. The Hg pulse cycles among surface reservoirs for decades through the legacy of storage in the subsurface ocean. We find a characteristic time scale of centuries for removal to ocean margin sediments versus thousands of years for removal to deep ocean sediments, so that ocean margin sediments are the dominant long-term sink of Hg. Unlike in Amos et al.,[46] the deep ocean does not become a dominant reservoir over centurial time scales because of the competing sink from ocean margin sediments.

Figure 4 shows the future recovery of the atmosphere and ocean under a hypothetical scenario of zero releases of primary
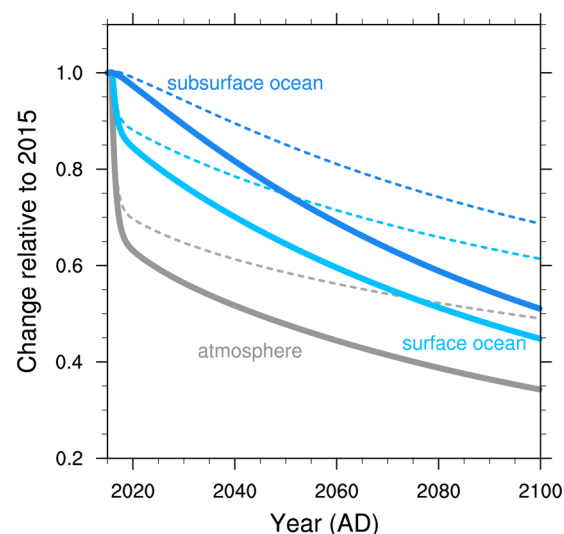
Figure 4. Change in global reservoir masses of Hg relative to 2015 under a hypothetical scenario of zero releases of primary anthropogenic Hg after 2015. Results are shown for the updated biogeochemical box model with sequestration in ocean margin sediments (solid) and without (dashed).

anthropogenic Hg after 2015. The effect of sequestration in ocean margin sediments is illustrated by comparing model results with and without this sink, where the latter is more similar to the original model version in Amos et al.[46] Sequestration in ocean margin sediments in our updated model hastens recovery in the atmosphere, surface, and subsurface ocean over the 21st century. The subsurface ocean decreases by 50% by 2100, as compared to 35% when we do not account for the sediment sink (Figure 4) and 25% in Amos et al.[46] Figure 4 also shows that the difference between simulations widens over time due to legacy Hg being more efficiently removed from active cycling.

Accounting for the additional loss of Hg to ocean margin sediments lowers the simulated steady-state natural budget of Hg in all reservoirs. This increases the relative perturbation from human activity and suggests an all-time relative enrichment in surface reservoirs possibly twice as large as previously estimated. Simulated natural deposition is 0.8 μg m^{-2} a^{-1}, which falls within the range of deposition in remote environments (0.6−1.7 μg m^{-2} a^{-1}) estimated from multi-millennia peat archives.[77] However, all-time enrichment is

sensitive to changes in the efficiency of long-term storage in terrestrial soils and sequestration in ocean margin sediments. Accelerated soil erosion through land-use change (e.g., deforestation and intensified agriculture) could affect long-term Hg storage in soils. The result would be a decrease in Hg accumulation in the ocean due to increasing burial at ocean margins. Benthic sediments at ocean margins have been highly perturbed by activities such as coastal development, dredging, and trawling.[78] Such disturbance would prolong the biogeochemical lifetime of anthropogenic Hg.

The analysis here points to multiple research needs. Repeated or continuous measurements of Hg concentrations, as well as dated sediment cores, near the mouths of major rivers in Asia are important for refining global estimates of Hg discharges to ocean margins and monitoring its direction of change. Observations from major rivers in Africa and South America would also help fill in major data gaps. In the context of global Hg cycling, better information is needed on the long-term fate of Hg in benthic ocean margin sediments.

■ ASSOCIATED CONTENT

Ⓢ Supporting Information

The Supplemental Information includes a complete compilation of present-day Hg measurements collected at or near river mouths and detailed descriptions of the data used to estimate regional Hg enrichment factors. This material is available free of charge via the Internet at http://pubs.acs.org.

■ AUTHOR INFORMATION

Corresponding Author

*Phone: (617) 496-5348; fax: (617) 495-4551; e-mail: hamos@hsph.harvard.edu.

Notes

The authors declare no competing financial interest.

■ ACKNOWLEDGMENTS

■ REFERENCES

(1) Mahaffey, K. R.; Sunderland, E. M.; Chan, H. M.; Choi, A. L.; Grandjean, P.; Marien, K.; Oken, E.; Sakamoto, M.; Schoeny, R.; Weihe, P.; Yan, C. H.; Yasutake, A. Balancing the benefits of n-3 polyunsaturated fatty acids and the risks of methylmercury exposure from fish consumption. *Nutr. Rev.* **2011**, *69* (9), 493−508.

(2) Strode, S. A.; Jaegle, L.; Jaffe, D. A.; Swartzendruber, P. C.; Selin, N. E.; Holmes, C.; Yantosca, R. M. Trans-Pacific transport of mercury. *J. Geophys. Res.: Atmos.* **2008**, *113* (D15), 12.

(3) Swartzendruber, P. C.; Jaffe, D. A.; Prestbo, E. M.; Weiss-Penzias, P.; Selin, N. E.; Park, R.; Jacob, D. J.; Strode, S.; Jaegle, L.

Observations of reactive gaseous mercury in the free troposphere at the Mount Bachelor Observatory. *J. Geophys. Res.: Atmos.* **2006**, *111* (D24), 12.

(4) Corbitt, E. S.; Jacob, D. J.; Holmes, C. D.; Streets, D. G.; Sunderland, E. M. Global source-receptor relationships for mercury deposition under present-day and 2050 emissions scenarios. *Environ. Sci. Technol.* **2011**, *45* (24), 10477−10484.

(5) Sunderland, E. M.; Krabbenhoft, D. P.; Moreau, J. W.; Strode, S. A.; Landing, W. M. Mercury sources, distribution, and bioavailability in the North Pacific Ocean: Insights from data and models. *Global Biogeochem. Cycle* **2009**, *23*, 14.

(6) AMAP/UNEP. *Technical Background Report for the Global Mercury Assessment 2013*; Arctic Monitoring and Assessment Program: Oslo, Norway/UNEP Chemicals Branch: Geneva, Switzerland, 2013; pp vi−263.

(7) AMAP/UNEP. *Technical Background Report to the Global Atmospheric Mercury Assessment*; Arctic Monitoring and Assessment Program: Oslo, Norway/UNEP Chemicals Branch: Geneva, Switzerland, 2008; p 159.

(8) Sunderland, E. M.; Mason, R. P. Human impacts on open ocean mercury concentrations. *Global Biogeochem. Cycles* **2007**, *21* (4), GB4022.

(9) Cossa, D.; Coquery, M.; Gobeil, C.; Martin, J. M. Mercury fluxes at the ocean margins. In *Global and Regional Mercury Cycles: Sources, Fluxes and Mass Balances*; Baeyens, W., Ebinghaus, R., Vasiliev, O., Eds.; Kluwer Academic Publishers: Amsterdam, The Netherlands, 1996; Vol. *21*, pp 229−247.

(10) Holmes, C. D.; Jacob, D. J.; Corbitt, E. S.; Mao, J.; Yang, X.; Talbot, R.; Slemr, F. Global atmospheric model for mercury including oxidation by bromine atoms. *Atmos. Chem. Phys.* **2010**, *10*, 12037−12057.

(11) Chester, R. The transport of material to the oceans: relative flux magnitudes. In *Marine Geochemistry*, 2nd ed.; Chester, R., Ed.; Blackwell Science: Oxford, U.K., 2003; pp 98−134.

(12) Cossa, D.; Martin, J. M.; Takayanagi, K.; Sanjuan, J. The distribution and cycling of mercury species in the western Mediterranean. *Deep Sea Res., Part II* **1997**, *44* (3−4), 721−740.

(13) Soerensen, A. L.; Jacob, D. J.; Streets, D. G.; Witt, M. L. I.; Ebinghaus, R.; Mason, R. P.; Andersson, M.; Sunderland, E. M. Multi-decadal decline of mercury in the North Atlantic atmosphere explained by changing subsurface seawater concentrations. *Geophys. Res. Lett.* **2012**, *39*, L21810.

(14) Fisher, J. A.; Jacob, D. J.; Soerensen, A. L.; Amos, H. M.; Steffen, A.; Sunderland, E. M. Riverine source of Arctic Ocean mercury inferred from atmospheric observations. *Nat. Geosci.* **2012**, *5* (7), 499−504.

(15) Kirk, J. L.; Lehnherr, I.; Andersson, M.; Braune, B. M.; Chan, L.; Dastoor, A. P.; Durnford, D.; Gleason, A. L.; Loseto, L. L.; Steffen, A.; St Louis, V. L. Mercury in Arctic marine ecosystems: Sources, pathways and exposure. *Environ. Res.* **2012**, *119*, 64−87.

(16) Dastoor, A. P.; Durnford, D. A. Arctic Ocean: Is it a sink or a source of atmospheric mercury? *Environ. Sci. Technol.* **2013**, *48* (3), 1707−1717.

(17) Mason, R. P.; Kim, E. H.; Cornwell, J. Metal accumulation in Baltimore Harbor: Current and past inputs. *Appl. Geochem.* **2004**, *19* (11), 1801−1825.

(18) Sunderland, E. M.; Gobas, F.; Heyes, A.; Branfireun, B. A.; Bayer, A. K.; Cranston, R. E.; Parsons, M. B. Speciation and bioavailability of mercury in well-mixed estuarine sediments. *Mar. Chem.* **2004**, *90* (1−4), 91−105.

(19) Schuster, P. F.; Striegl, R. G.; Aiken, G. R.; Krabbenhoft, D. P.; Dewild, J. F.; Butler, K.; Kamark, B.; Dornblaser, M. Mercury export from the Yukon River Basin and potential response to a changing climate. *Environ. Sci. Technol.* **2011**, *45* (21), 9262−9267.

(20) McKee, B. A.; Aller, R. C.; Allison, M. A.; Bianchi, T. S.; Kineke, G. C. Transport and transformation of dissolved and particulate materials on continental margins influenced by major rivers: Benthic boundary layer and seabed processes. *Cont. Shelf Res.* **2004**, *24* (7−8), 899−926.

9520

dx.doi.org/10.1021/es502134t | *Environ. Sci. Technol.* 2014, 48, 9514−9522

(21) Walsh, J. P.; Nittrouer, C. A. Understanding fine-grained river-sediment dispersal on continental margins. *Mar. Geol.* **2009**, *263* (1−4), 34−45.

(22) Gill, G. A.; Fitzgerald, W. F. Vertical mercury distributions in the oceans. *Geochim. Cosmochim. Acta* **1988**, *52* (6), 1719−1728.

(23) Mason, R. P.; Choi, A. L.; Fitzgerald, W. F.; Hammerschmidt, C. R.; Lamborg, C. H.; Soerensen, A. L.; Sunderland, E. M. Mercury biogeochemical cycling in the ocean and policy implications. *Environ. Res.* **2012**, *119*, 101−117.

(24) Mason, R. P.; Lawson, N. M.; Sheu, G. R. Mercury in the Atlantic Ocean: Factors controlling air-sea exchange of mercury and its distribution in the upper waters. *Deep Sea Res., Part II* **2001**, *48* (13), 2829−2853.

(25) Bopp, R. F.; Simpson, H. J.; Chillrud, S. N.; Robinson, D. W. Sediment-derived chronologies of persistent contaminants in Jamaica Bay, New York. *Estuaries* **1993**, *16* (3B), 608−616.

(26) Steinberg, N.; Suszkowski, D. J.; Clark, L.; Way, J. *Health of the Harbor: The First Comprehensive Look at the State of the NY/NJ. Harbor Estuary*; Hudson River Foundation: New York, 2004; p 22.

(27) Mansson, N.; Bergback, B.; Sorme, L. Phasing out cadmium, lead, and mercury. *J. Ind. Ecol.* **2009**, *13* (1), 94−111.

(28) Harland, B. J.; Taylor, D.; Wither, K. The distribution of mercury and other trace metals in the sediments of the Mersey Estuary over 25 years 1974−1998. *Sci. Total Environ.* **2000**, *253* (1−3), 45−62.

(29) Leermakers, M.; Galletti, S.; De Galan, S.; Brion, N.; Baeyens, W. Mercury in the southern North Sea and Scheldt estuary. *Mar. Chem.* **2001**, *75* (3), 229−248.

(30) Varekamp, J. C.; Kreulen, B.; ten Brink, M. R. B.; Mecray, E. L. Mercury contamination chronologies from Connecticut wetlands and Long Island Sound sediments. *Environ. Geol.* **2003**, *43* (3), 268−282.

(31) An, Q.; Wu, Y. Q.; Wang, J. H.; Li, Z. E. Assessment of dissolved heavy metal in the Yangtze River estuary and its adjacent sea, China. *Environ. Monit. Assess.* **2010**, *164* (1−4), 173−187.

(32) Ram, A.; Rokade, M. A.; Borole, D. V.; Zingde, M. D. Mercury in sediments of Ulhas estuary. *Mar. Pollut. Bull.* **2003**, *46* (7), 846−857.

(33) Chakraborty, L. B.; Qureshi, A.; Vadenbo, C.; Hellweg, S. Anthropogenic mercury flows in India and impacts of emission controls. *Environ. Sci. Technol.* **2013**, *47* (15), 8105−8113.

(34) Cossa, D.; Coquery, M. The Mediterranean mercury anomaly, a geochemical or a biological issue. *Mediterr. Sea* **2005**, *5*, 177−208.

(35) Ludwig, W.; Amiotte-Suchet, P.; Probst, J. L. ISLSCP II global river fluxes of carbon and sediments to the oceans. In *ISLSCP Initiative II Collection. Data Set.*; Hall, F. G., Collatz, G., Meeson, B., Los, S., Brown de Colstoun, E., Landis, D., Eds.; Oak Ridge Natinal Laboratory Distributed Active Archive Center: Oak Ridge, TN, 2011.

(36) Ludwig, W.; Probst, J. L.; Kempe, S. Predicting the oceanic input of organic carbon by continental erosion. *Global Biogeochem. Cycle* **1996**, *10* (1), 23−41.

(37) Hall, F. G.; de Colstoun, E. B.; Collatz, G. J.; Landis, D.; Dirmeyer, P.; Betts, A.; Huffman, G. J.; Bounoua, L.; Meeson, B. ISLSCP Initiative II global data sets: Surface boundary conditions and atmospheric forcings for land-atmosphere studies. *J. Geophys. Res.: Atmos.* **2006**, *111*, D22.

(38) Dai, A.; Qian, T. T.; Trenberth, K. E.; Milliman, J. D. Changes in continental freshwater discharge from 1948 to 2004. *J. Clim.* **2009**, *22* (10), 2773−2792.

(39) Zhang, Y.; Jacob, D. J.; Amos, H. M.; Sunderland, E. M. Transport and fate of riverine discharged mercury in the ocean: Insights from a 3D transport model. **2014**, in preparation.

(40) Tomiyasu, T.; Matsuyama, A.; Eguchi, T.; Fuchigami, Y.; Oki, K.; Horvat, M.; Rajar, R.; Akagi, H. Spatial variations of mercury in sediment of Minamata Bay, Japan. *Sci. Total Environ.* **2006**, *368* (1), 283−290.

(41) Marshall, J.; Hill, C.; Perelman, L.; Adcroft, A. Hydrostatic, quasi-hydrostatic, and nonhydrostatic ocean modeling. *J. Geophys. Res.: Oceans* **1997**, *102* (C3), 5733−5752.

(42) Soerensen, A. L.; Sunderland, E. M.; Holmes, C. D.; Jacob, D. J.; Yantosca, R. M.; Skov, H.; Christensen, J. H.; Strode, S. A.; Mason, R.

P. An improved global model for air-sea exchange of mercury: High concentrations over the North Atlantic. *Environ. Sci. Technol.* **2010**, *44* (22), 8574−8580.

(43) Zhang, Y.; Jaegle, L.; Thompson, L. Natural biogeochemical cycle of mercury in a global three-dimensional ocean tracer model. *Global. Biogeochem. Cycle* **2014**, *28* (5), 553−570.

(44) Dutkiewicz, S.; Ward, B. A.; Monteiro, F.; Follows, M. J. Interconnection of nitrogen fixers and iron in the Pacific Ocean: Theory and numerical simulations. *Global Biogeochem. Cycle* **2012**, *26*, 16.

(45) Wunsch, C.; Heimbach, P. Practical global oceanic state estimation. *Phys. D (Amsterdam, Neth.)* **2007**, *230* (1−2), 197−208.

(46) Amos, H. M.; Jacob, D. J.; Streets, D. G.; Sunderland, E. M. Legacy impacts of all-time anthropogenic emissions on the global mercury cycle. *Global Biogeochem. Cycle* **2013**, *27* (2), 410−421.

(47) Streets, D. G.; Devane, M. K.; Lu, Z. F.; Bond, T. C.; Sunderland, E. M.; Jacob, D. J. All-time releases of mercury to the atmosphere from human activities. *Environ. Sci. Technol.* **2011**, *45* (24), 10485−10491.

(48) Horowitz, H. M.; Jacob, D. J.; Amos, H. M.; Streets, D. G.; Sunderland, E. M. Historical mercury releases from commercial products: Global environmental implications. *Environ. Sci. Technol.* **2014**, submitted for publication.

(49) Hararuk, O.; Obrist, D.; Luo, Y. Modelling the sensitivity of soil mercury storage to climate-induced changes in soil carbon pools. *Biogeosciences* **2013**, *10* (4), 2393−2407.

(50) Obrist, D.; Pokharel, A. K.; Moore, C. Vertical profile measurements of soil air suggest immobilization of gaseous elemental mercury in mineral soil. *Environ. Sci. Technol.* **2014**, *48* (4), 2242−2252.

(51) Obrist, D. Mercury distribution across 14 U.S. forests. Part II: Patterns of methyl mercury concentrations and areal mass of total and methyl mercury. *Environ. Sci. Technol.* **2012**, *46* (11), 5921−5930.

(52) Leitch, D. R.; Carrie, J.; Lean, D.; Macdonald, R. W.; Stern, G. A.; Wang, F. Y. The delivery of mercury to the Beaufort Sea of the Arctic Ocean by the Mackenzie River. *Sci. Total Environ.* **2007**, *373* (1), 178−195.

(53) Emmerton, C. A.; Graydon, J. A.; Gareis, J. A. L.; St Louis, V. L.; Lesack, L. F. W.; Banack, J. K. A.; Hicks, F.; Nafziger, J. Mercury export to the Arctic Ocean from the Mackenzie River, Canada. *Environ. Sci. Technol.* **2013**, *47* (14), 7644−7654.

(54) Bi, C. J.; Chen, Z. L.; Shen, J.; Sun, W. W. Variations of mercury distribution in the water column during the course of a tidal cycle in the Yangtze Estuarine intertidal zone, China. *Sci. China: Chem.* **2012**, *55* (10), 2224−2232.

(55) Jiang, H.; Feng, X.; Dai, Q.; Tao, F.; Liu, C. The distribution and speciation of mercury in Wujiang river. *J. Phys. IV* **2003**, *107*, 679−682.

(56) Liu, J. L.; Feng, X. B.; Zhu, W.; Zhang, X.; Yin, R. S. Spatial distribution and speciation of mercury and methyl mercury in the surface water of East River (Dongjiang) tributary of Pearl River Delta, South China. *Environ. Sci. Pollut. Res.* **2012**, *19* (1), 105−112.

(57) Tong, Y. D.; Zhang, W.; Hu, D.; Ou, L. B.; Hu, X. D.; Yang, T. J.; Wei, W.; Ju, L.; Wang, X. J. Behavior of mercury in an urban river and its accumulation in aquatic plants. *Environ. Earth Sci.* **2013**, *68* (4), 1089−1097.

(58) Sankar, R.; Ramkumar, L.; Rajkumar, M.; Sun, J.; Ananthan, G. Seasonal variations in physico-chemical parameters and heavy metals in water and sediments of Uppanar estuary, Nagapattinam, India. *J. Environ. Biol.* **2010**, *31* (5), 681−686.

(59) Quemerais, B.; Cossa, D.; Rondeau, B.; Pham, T. T.; Gagnon, P.; Fortin, B. Sources and fluxes of mercury in the St. Lawrence river. *Environ. Sci. Technol.* **1999**, *33* (6), 840−849.

(60) Outridge, P. M.; Macdonald, R. W.; Wang, F.; Stern, G. A.; Dastoor, A. P. A mass balance inventory of mercury in the Arctic Ocean. *Environ. Chem.* **2008**, *5* (2), 89−111.

(61) Rajar, R.; Cetina, M.; Horvat, M.; Zagar, D. Mass balance of mercury in the Mediterranean Sea. *Mar. Chem.* **2007**, *107* (1), 89−102.

(62) UNEP. *Guinea Current, GIWA Regional Assessment 42*; University of Kalamar: Kalamar, Sweden, 2004.

(63) Wright, L. D.; Wiseman, W. J.; Bornhold, B. D.; Prior, D. B.; Suhayda, J. N.; Keller, G. H.; Yang, Z. S.; Fan, Y. B. Marine dispersal and deposition of Yellow River silts by gravity-driven underflows. *Nature* **1988**, *332* (6165), 629−632.

(64) Milliman, J. D.; Farnsworth, K. L. Runoff, erosion, and delivery to the coastal ocean. In *River Discharge to the Coastal Ocean: A Global Synthesis*; Cambridge University Press: New York, 2011; pp 13−61.

(65) Cossa, D.; Heimburger, L. E.; Lannuzel, D.; Rintoul, S. R.; Butler, E. C. V.; Bowie, A. R.; Averty, B.; Watson, R. J.; Remenyi, T. Mercury in the Southern Ocean. *Geochim. Cosmochim. Acta* **2011**, *75* (14), 4037−4052.

(66) Blum, J. D.; Popp, B. N.; Drazen, J. C.; Choy, C. N.; Johnson, M. W. Methylmercury production below the mixed layer in the North Pacific Ocean. *Nat. Geosci.* **2013**, *6*, 879−884.

(67) Cossa, D.; Averty, B.; Pirrone, N. The origin of methylmercury in open Mediterranean waters. *Limnol. Oceanogr.* **2009**, *54*, 837−844.

(68) Maxson, P. *Mercury Flows in Europe and the World: Impact of Decommissioned Chlor-alkali Plants*; European Commission, Directorate General for Environment: Brussels, Belgium, 2004; p 104.

(69) Hylander, L. D.; Meili, M. The rise and fall of mercury: Converting a resource to refuse after 500 years of mining and pollution. *Crit. Rev. Environ. Sci. Technol.* **2005**, *35* (1), 1−36.

(70) Wilburn, D. R. *Changing Patterns in the Use, Recycling, and Material Substitution of Mercury in the United States*; U. S. Geological Survey: Reston, VA, 2013; p 32.

(71) Shi, J. B.; Ip, C. C. M.; Zhang, G.; Jiang, G. B.; Li, X. D. Mercury profiles in sediments of the Pearl River Estuary and the surrounding coastal area of South China. *Environ. Pollut.* **2010**, *158* (5), 1974−1979.

(72) Liu, J. G.; Yang, W. Water sustainability for China and beyond. *Science* **2012**, *337* (6095), 649−650.

(73) Yi, Y. J.; Yang, Z. F.; Zhang, S. H. Ecological risk assessment of heavy metals in sediment and human health risk assessment of heavy metals in fishes in the middle and lower reaches of the Yangtze River basin. *Environ. Pollut.* **2011**, *159* (10), 2575−2585.

(74) Pacyna, E. G.; Pacyna, J. M.; Sundseth, K.; Munthe, J.; Kindbom, K.; Wilson, S.; Steenhuisen, F.; Maxson, P. Global emission of mercury to the atmosphere from anthropogenic sources in 2005 and projections to 2020. *Atmos. Environ.* **2010**, *44* (20), 2487−2499.

(75) Maxson, P. *Mercury Flows and Safe Storage of Surplus Mercury*; European Commission Directorate General for Environment: Brussels, Belgium, 2006; p 71.

(76) Zhang, H.; Shan, B. Historical records of heavy metal accumulation in sediments and the relationship with agricultural intensification in the Yangtze−Huaihe region, China. *Sci. Total Environ.* **2008**, *399* (1−3), 113−120.

(77) Biester, H.; Bindler, R.; Martinez-Cortizas, A.; Engstrom, D. R. Modeling the past atmospheric deposition of mercury using natural archives. *Environ. Sci. Technol.* **2007**, *41* (14), 4851−4860.

(78) Mayer, L. M.; Schick, D. F.; Findlay, R. H.; Rice, D. L. Effects of commercial dragging on sedimentary organic matter. *Mar. Environ. Res.* **1991**, *31* (4), 249−261.

(79) Gatz, D. F.; Smith, L. The standard error of a weighted mean concentration. 1. Bootstrapping vs other methods. *Atmos. Environ.* **1995**, *29* (11), 1185−1193.

(80) Noh, S.; Choi, M.; Kim, E.; Dan, N. P.; Thanh, B. X.; Ha, N. T. V.; Sthiannopkao, S.; Han, S. Influence of salinity intrusion on the speciation and partitioning of mercury in the Mekong River Delta. *Geochim. Cosmochim. Acta* **2013**, *106*, 379−390.

9522

dx.doi.org/10.1021/es502134t | *Environ. Sci. Technol.* 2014, 48, 9514−9522